

Supporting Information

Undurraga et al. 10.1073/pnas.1211021109

SI Materials and Methods

Plant Materials and Growth Conditions. The 181 *Arabidopsis thaliana* accessions are as previously described (1). The loss-of-function *EARLY FLOWERING 3* (*elf3*) mutants are: (i) *elf3-4*, containing a *CCR2::LUC* transgene (ecotype Ws) (2, 3) and (ii) *elf3-200*, the GABI750E02 T-DNA insertion mutant (ecotype Col-0) (4). For hypocotyl experiments, seeds were sterilized with Ethanol and plated onto 1× Murashige and Skoog (MS) basal salt medium supplemented with 1× MS vitamins, 1% (wt/vol) sucrose, 0.05% Mes (wt/vol), and 0.24% (wt/vol) phytigel. After stratification in the dark at 4 °C for 3 d, plates were transferred to an incubator (Conviron) that was set to either short day (SD) (8L:16D at 20 °C) or long day (LD) (16L:8D at 22 °C:20 °C), with light supplied at 100 μmol·m⁻²·s⁻¹ by cool-white fluorescent bulbs. For growth on soil, seeds were stratified at 4 °C for 3 d, and then grown in Sunshine #4 soil under cool-white fluorescent light at either LD or SD at 20 °C. Seedlings used for RNA extractions were grown on soil under LD conditions and harvested on day 10. Samples for *ELF3* expression measurements were collected at Zeitgeber time (ZT) 20. Samples for *Phytochrome-interacting Factor 5* (*PIF5*) expression measurements were collected at ZT 8. Samples for and *Pseudoresponse regulator 9* (*PRR9*) expression measurements were collected at ZT 0, 5, and 8.

Generation of *ELF3* Transgenic Plants. To generate *A. thaliana* transgenics carrying different *ELF3 tandem repeat* (*TR*) alleles, the cDNA clone RAFL09-28-E05 (RIKEN BRC) (5, 6), containing the *ELF3* coding region and 3' UTR (Col-0 accession) was used. This cDNA clone lacks the small 5' intron. Two restriction sites, NarI and NcoI, were inserted into the *ELF3* coding sequence using the QuikChange Site-Directed Mutagenesis kit (Stratagene) (primer information in Table S5). The polyglutamine (polyQ)-encoding region was amplified from accessions containing selected TR copy number alleles (primer information in Table S5, TR allele information in Table S1). These PCR products were digested with NarI/NcoI and ligated into the previously mutagenized *ELF3* coding region. An artificial allele lacking the TR was generated by site-directed mutagenesis (primer information in Table S5). Mutated plasmids and all ligation products were sequenced to ensure accuracy. The *ELF3* alleles were cloned into pENTR1A (Invitrogen). A 2-kbp NotI fragment containing the *ELF3* promoter was inserted upstream of each *ELF3* coding sequence. The fragments containing the *ELF3* promoter, *ELF3* coding sequence, and the *ELF3* 3' UTR were recombined using Gateway LR Clonase II (Invitrogen) into a modified pB7WG2 (7), which lacks the CaMV-35S promoter. The region encoding the polyQ tract of each construct was sequenced to ensure accurate TR copy number. The plasmids were used to transform *Agrobacterium tumefaciens* GV3101. Subsequently, *Arabidopsis elf3* mutants were transformed by the flower dip method (8). Transformants were selected on Basta (Liberty herbicide; Bayer Crop Science) and propagated for three to four generations. The accuracy of the transgenes was confirmed by PCR (primer information in Table S5). All Ws phenotypic assays were performed in homozygous transgenic plants with expression levels between 0.8- and 4.5-times the respective *ELF3* wild-type (Fig. S1C); for Col lines, transgene expression levels were between 0.3- and 4.3-times the respective *ELF3* wild-type (Fig. S1D). Analyzed plant lines are in Tables S2–S4.

RNA Extractions and Real-Time PCR. Total RNA was extracted from 30-mg frozen tissue using the SV Total RNA Isolation System (Promega). Subsequently, 2 μg of RNA were subjected to DNase treatment using Ambion Turbo DNA-free Kit (Applied Biosystems). RNA integrity and purity were checked with an Agilent Bioanalyzer using the RNA 6000 Nano Kit (Agilent Technologies). For cDNA synthesis, 200 ng of DNase-treated RNA was reverse-transcribed using the Transcriptor First Strand cDNA Synthesis Kit (Roche) and oligo dT primers. Transcript abundance was determined by real-time quantitative PCR using the LightCycler 480 system (Roche), with LightCycler 480 SYBR Green I Master (Roche) and the following PCR conditions: 5 min at 95 °C, followed by 35 cycles of 15 s at 95 °C, 20 s at 55 °C, and 20 s at 72 °C. To ensure that PCR products were unique, a melting-curve analysis was performed after the amplification. *UBC21* expression (At5g25760) was used as a reference. All quantitative RT-PCR primers were designed with the LightCycler Probe Design Software (Roche). Sequences for real-time PCR primers are shown in Table S6. Relative quantification was determined with the $\Delta\Delta CT$ Method (9). Error was calculated as previously described (10).

Thermal Asymmetric Interlaced PCR. High-efficiency thermal asymmetric interlaced (TAIL)-PCR was performed as previously described (11) to obtain the flanking sequence of the construct integration site (left border). Briefly, a preamplification step was performed with primers LAD and LB-0a (Table S7), followed by primary TAIL-PCR with primers AC1 (11) and LB-1a (Table S7), and 1 μL of a 1/40 dilution of the preamplification product as a template. A secondary TAIL-PCR with primers AC2 (11) and LB-2a (Table S7) was performed with 1 μL of a 1/10 dilution of the primary TAIL-PCR product. Next, 3-kbp products were extracted from agarose gels and subsequently Sanger-sequenced. Only sequences containing the T-DNA left border were considered.

Developmental Phenotype Assays. For measurements of hypocotyl length, seedlings were grown on vertical plates for 15 d in a pseudorandomized design under either SD or LD conditions (12). Hypocotyl length was measured with ImageJ on digital images (<http://rsbweb.nih.gov/ij/>). For measurement of flowering time, seeds were planted in sheet pots (36 pots per tray) in a randomized design and trays were rotated daily. Flowering time was recorded as the day when the inflorescence reached 1 cm in height. Rosette leaf number was determined on the same day. Petiole-length/leaf-length (PL/LL) ratio for leaf four was determined on day 45. Least-square means for all traits were derived from a linear regression analysis for each trait separately. *ELF3 TR* copy number was modeled as a nominal variable and independent transgenic lines carrying the same *ELF3 TR* allele were analyzed together. We tested for significant phenotypic differences conferred by the different *ELF3 TR* alleles by using Tukey-HSD tests with $\alpha = 0.05$ that accommodate nonnormal data.

Luciferase Imaging and Period Analysis. Luciferase assays were performed with lines containing the *CCR2::LUC* reporter. Seeds were surface sterilized with a 70% (vol/vol) ethanol wash followed by a second wash with 33% (vol/vol) Klorix with Triton X-100, and then rinsed twice with sterile water. Seeds were plated on MS3 medium [pH 5.7, 3% (wt/vol) sucrose, 1.5% (wt/vol) PhytoAgar, and 15 μg/mL hygromycin B]. They were subsequently stratified for 4 d at 4 °C in the dark and entrained under 12-h light:12-h dark cycles under white fluorescent light (~10 μmol·m⁻²·s⁻¹) at 22 °C.

On the sixth day, a minimum of 24 seedlings per line was transferred to 96-well TopCount (Perkin-Elmer) plates containing 200 μL MS3 agar. We added 5 mM Luciferin in 0.01% Triton X-100 and entrained seedlings for another cycle before luminescence was detected using a Packard/Perkin-Elmer TopCount Scintillation and Luminescence Counter. Red and blue light-emitting diodes ($\sim 2 \mu\text{mol}\cdot\text{m}^{-2}\cdot\text{s}^{-1}$) were used as a light source during this analysis. During the first 24 h of luminescence detection, plants were grown in 12-h light:12-h dark and then released under constant light conditions to measure the free-running period. Each individual was measured approximately every 30 min for a minimum of 5 d. Luminescence levels were quantified and analyzed as previously described (2, 3) using the macro suites TopTempII and Biological Rhythms Analysis Software System (13). Period length and relative amplitude error (RAE) were estimated using fast Fourier transform nonlinear least squares (14). Period values scored with RAE values below 0.4 were considered robustly rhythmic (15).

Principal Components Analysis. We clustered our phenotypic data using principal components analysis (PCA) to find patterns corresponding to genotypes. We excluded the phenotype of rosette leaf number in SD, for which data were missing for several alleles. The phenotypes included in the analysis are: Days to flowering in SD and LD conditions, hypocotyl length under SD

and LD PL/LL for the fourth leaf in SD, and rosette leaf number in LD. For analyses involving Col lines, the SD PL/LL ratio phenotype was omitted because of lack of data, and PCA was thus based on the remaining five phenotypic variables. For each phenotype in each genetic background (either Ws or Col-0), we calculated the mean phenotype of the independently generated lines for each *ELF3-TR* allele, giving us a 28×6 matrix of mean phenotypes for the 28 genotypes for each of six phenotypic variables. Within each background, we ranked the genotypes for each phenotype. Ranks were transformed into a standard normal distribution based on their percentile, using the R function *qnorm*. Using this transformed dataset, we performed PCA using the R function *prcomp* (R Foundation for Statistical Computing, <http://www.r-project.org/>, 2011). We performed PCA for each background separately, and then for both backgrounds together. Rank-normalization was necessary to compare (i) phenotypes measured on different scales and (ii) Ws- and Col-derived plants, between which backgrounds absolute phenotypic differences exist. Consequently, the rank-normalization increases stability of our estimates, as our dataset is relatively small and PCA's assumptions of normality were not met by our raw dataset. PCA on raw values scaled to a standard normal distribution gave similar results. Biplots were generated with the R *biplot* function on *prcomp* function output.

- Shindo C, et al. (2005) Role of FRIGIDA and FLOWERING LOCUS C in determining variation in flowering time of *Arabidopsis*. *Plant Physiol* 138(2):1163–1173.
- Covington MF, et al. (2001) ELF3 modulates resetting of the circadian clock in *Arabidopsis*. *Plant Cell* 13(6):1305–1315.
- Doyle MR, et al. (2002) The ELF4 gene controls circadian rhythms and flowering time in *Arabidopsis thaliana*. *Nature* 419(6902):74–77.
- Rosso MG, et al. (2003) An *Arabidopsis thaliana* T-DNA mutagenized population (GABI-Kat) for flanking sequence tag-based reverse genetics. *Plant Mol Biol* 53(1–2):247–259.
- Seki M, Carninci P, Nishiyama Y, Hayashizaki Y, Shinozaki K (1998) High-efficiency cloning of *Arabidopsis* full-length cDNA by biotinylated CAP trapper. *Plant J* 15(5):707–720.
- Seki M, et al. (2002) Functional annotation of a full-length *Arabidopsis* cDNA collection. *Science* 296(5565):141–145.
- Karimi M, Inzé D, Depicker A (2002) GATEWAY vectors for *Agrobacterium*-mediated plant transformation. *Trends Plant Sci* 7(5):193–195.
- Clough SJ, Bent AF (1998) Floral dip: A simplified method for *Agrobacterium*-mediated transformation of *Arabidopsis thaliana*. *Plant J* 16(6):735–743.
- Livak KJ, Schmittgen TD (2001) Analysis of relative gene expression data using real-time quantitative PCR and the $2^{-\Delta\Delta CT}$ method. *Methods* 25(4):402–408.
- Specchia V, et al. (2010) Hsp90 prevents phenotypic variation by suppressing the mutagenic activity of transposons. *Nature* 463(7281):662–665.
- Liu YG, Chen Y (2007) High-efficiency thermal asymmetric interlaced PCR for amplification of unknown flanking sequences. *Biotechniques* 43(5):649–650, 652, 654 passim.
- Sangster TA, et al. (2008) HSP90 affects the expression of genetic variation and developmental stability in quantitative traits. *Proc Natl Acad Sci USA* 105(8):2963–2968.
- Southern MM, Millar AJ (2005) Circadian genetics in the model higher plant, *Arabidopsis thaliana*. *Methods Enzymol* 393:23–35.
- Plautz JD, et al. (1997) Quantitative analysis of *Drosophila* period gene transcription in living animals. *J Biol Rhythms* 12(3):204–217.
- Izumo M, Sato TR, Straume M, Johnson CH (2006) Quantitative analyses of circadian gene expression in mammalian cell cultures. *PLOS Comput Biol* 2(10):e136.

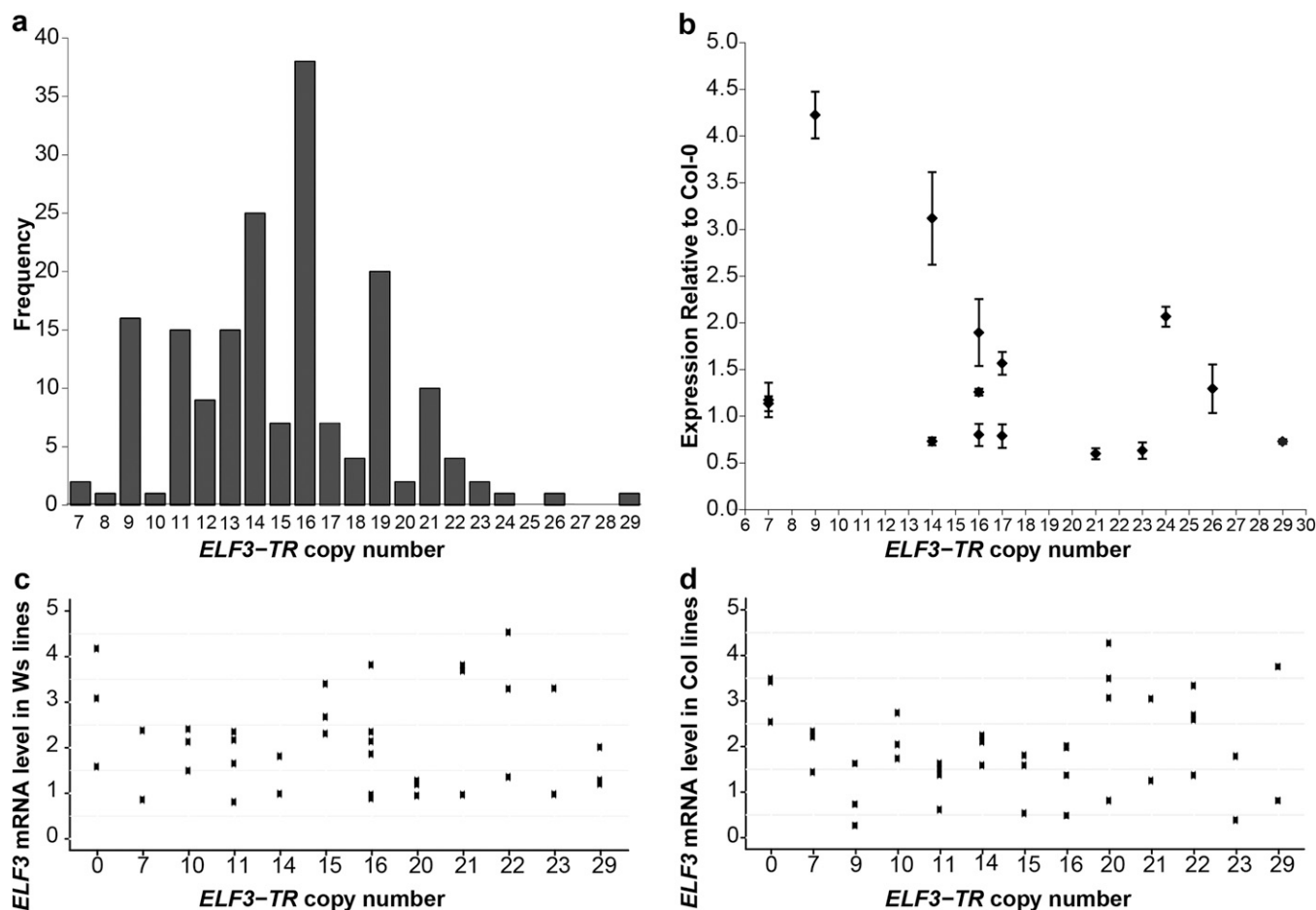


Fig. S1. The *ELF3-TR* variation is not correlated with *ELF3* expression. (A) Histogram of *ELF3-TR* copy number across 181 accessions. TR copy number was determined by Sanger sequencing. (B) *ELF3* expression levels in selected natural accessions were measured by quantitative RT-PCR. Expression values are given relative to the Col-0 wild-type reference. Three biological replicates with three technical replicates each were used to obtain expression values. Bars indicate \pm SEM. (C and D) *ELF3-TR* transgenic lines are expression-matched in both genetic backgrounds. (C) *elf3-4*, Ws; (D) *elf3-200*, Col. *ELF3* mRNA levels were measured by quantitative PCR (for primers see Table S6) in pooled 10-d-old seedlings that were grown under LD and collected at ZT 20 for each independently generated *ELF3-TR* transgenic line. *ELF3* expression levels are shown relative to either Ws (C) or Col-0 (D) wild-types. Because *ELF3* expression levels are known to substantially affect *ELF3*-dependent phenotypes (1), *ELF3* expression is an important variable to consider in our assessment of polyQ tract-length effects. We made efforts to consider only lines within a certain range of *ELF3* expression and to test multiple independent lines per *ELF3-TR* allele (Tables S2–S4), but because of the technical constraints of transgenic plant construction, we cannot entirely exclude the possibility that *ELF3* expression partially explains our observations. Although the effects of both *ELF3* expression level and *ELF3-TR* copy number were highly significant, they appear to be largely independent. For example, the *ELF3-23Q* and *ELF3-16Q* alleles, which were among the most distinct *ELF3-TR* alleles in both backgrounds, had very similar ranges of *ELF3* expression. In Ws, the alleles *ELF3-7Q*, *ELF3-23Q*, and *ELF3-10Q* phenocopied an *elf3* loss-of-function mutant for some phenotypes. Their *ELF3* expression levels, however, were very similar to the *ELF3-16Q* allele, which complemented many *ELF3* functions in *elf3-4*. To formally address the contributions of *ELF3* expression and *ELF3-TR* copy number to phenotype, we performed a linear-regression analysis, in which we modeled the trait days to flower (SD) as a function of *ELF3-TR* copy number as a multilevel factorial variable and *ELF3* mRNA levels for transgenic lines as a covariate. *ELF3* expression and *ELF3-TR* copy number were both highly significant ($P < 0.0001$). This full model explained 46% of the observed phenotypic variance, whereas in models including either *ELF3* expression or *ELF3-TR* copy number as variables, only 18% or 26% of the phenotypic variance was explained. Contributions of *ELF3* expression and *ELF3-TR* copy number to other phenotypes were similar. As observed with individual *ELF3-TR* alleles, the phenotypic effects of *ELF3* expression levels appear to be largely independent of *ELF3-TR* copy number, which consistently explained a larger portion of phenotypic variation. Both variables showed significant interaction effects in a linear regression model, yet the coefficients for the interactions of specific *ELF3-TR* alleles with *ELF3* expression were both positive and negative. This finding indicates that *ELF3-TR* copy number may in fact modulate or buffer the effects of *ELF3* expression; however, our dataset is too small and biased toward similar expression values to confidently support this conclusion. In summary, we reject the hypothesis that our observations of phenotypic effects of *ELF3-TR* copy number variation are a trivial result of *ELF3* expression differences between lines.

1. Kim W-Y, Hicks KA, Somers DE (2005) Independent roles for *EARLY FLOWERING 3* and *ZEITLUPE* in the control of circadian timing, hypocotyl length, and flowering time. *Plant Physiol* 139(3):1557–1569.

(H and I) PCA of phenotypic data for all *ELF3-TR* alleles in the *elf3-4* background (Ws accession). (H) Biplot of PC1 and PC2, graphically showing the contribution of phenotypes to PCs as red arrows. Note that for the biplot representation, PC1 and PC2 are transformed to the same scale (bottom and left axes), whereas phenotype contributions (in red) are allowed to differ in scale (top and right axes). Phenotypes are hypocotyl length in short and long days (SD_hylen and LD_hylen), DTF in short and long days (SD_DTF and LD_DTF), and FLN in long days (LD_rosette). Wild-type plants are characterized by late flowering (large SD and LD_DTF, many rosette leaves) and short hypocotyls (small SD and LD_hylen), relative to *elf3* loss-of-function mutants. (I) PC1 and PC2. (J) PCA loadings for Ws background. hylen, hypocotyl length (mm). PCA loadings describe the composition of a principal component [i.e., the contribution of each phenotype in calculating the principal component, and the direction of a phenotype's contribution (the sign of the loading)]. For PC1, flowering-time phenotypes and circadian clock phenotypes have opposite loading signs, describing the tendency of late-flowering plants to have short hypocotyls (and short petioles; i.e., to be wild-type for all phenotypes).

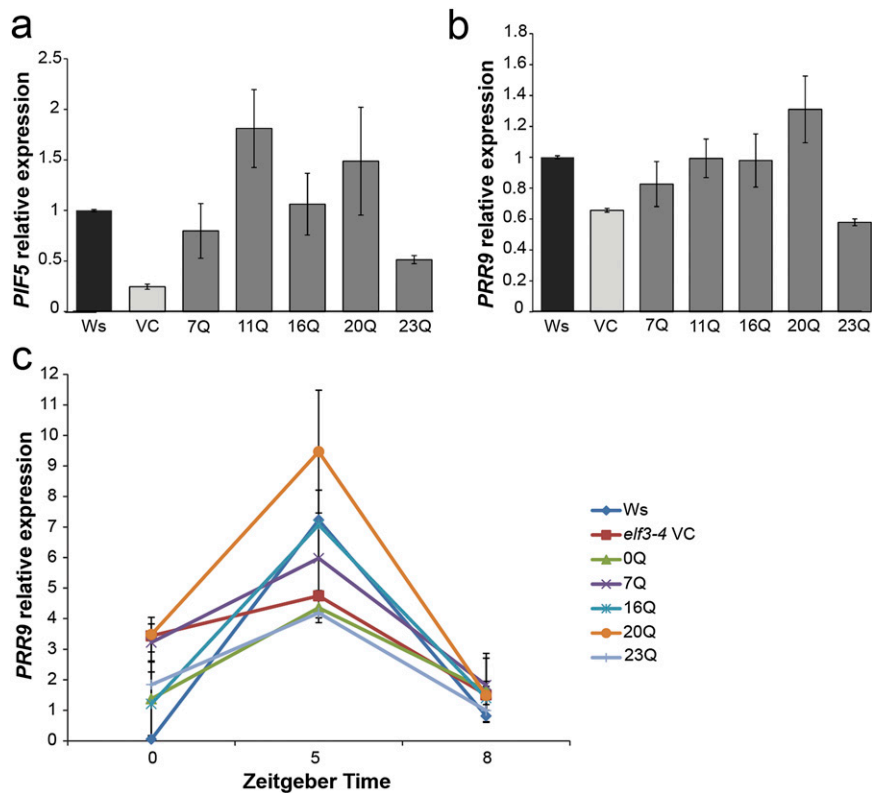


Fig. S3. Expression levels of the *ELF3*-regulated genes *PIF5* (A) and *PRR9* (B and C). Plants were grown under LD and RNA was collected at times showing the largest expression difference between wild-type and *elf3-4* mutant ZT8 for *PIF5* (1) (A) and ZT5 for *PRR9* (2, 3) (B and C). RNA levels were normalized relative to Ws wild-type. (C) Temporal variation in *PRR9* expression across *ELF3-TR* transgenic lines. *PRR9* expression levels were measured in 10-d-old plants grown under LD. RNA was collected at times demonstrating the diurnal oscillation of *PRR9* expression in wild-type, as determined previously (2, 3). RNA levels were normalized relative to wild-type (Ws) at ZT8. Gene expression was measured in triplicate for each biological replicate, with multiple independent transgenic lines as biological replicates for each *ELF3* allele. Error bars indicate SE of expression across biological replicates. Our expression patterns of *PRR9* for wild-type and the *elf3-4* mutant are similar to previous observations (2, 3). *ELF3-TR* alleles are indicated with the number of Qs encoded, Ws is wild-type, VC is the *elf3-4* vector control. Error bars are SEs of means. Data are from multiple independently generated expression-matched (Fig. S1C) T3 and T4 lines for each TR copy number allele (Table S2).

- Nusinow DA, et al. (2011) The ELF4-ELF3-LUX complex links the circadian clock to diurnal control of hypocotyl growth. *Nature* 475(7356):398–402.
- Kolmos E, et al. (2011) A reduced-function allele reveals that *EARLY FLOWERING3* repressive action on the circadian clock is modulated by phytochrome signals in *Arabidopsis*. *Plant Cell* 23(9):3230–3246.
- Dixon LE, et al. (2011) Temporal repression of core circadian genes is mediated through *EARLY FLOWERING 3* in *Arabidopsis*. *Curr Biol* 21(2):120–125.

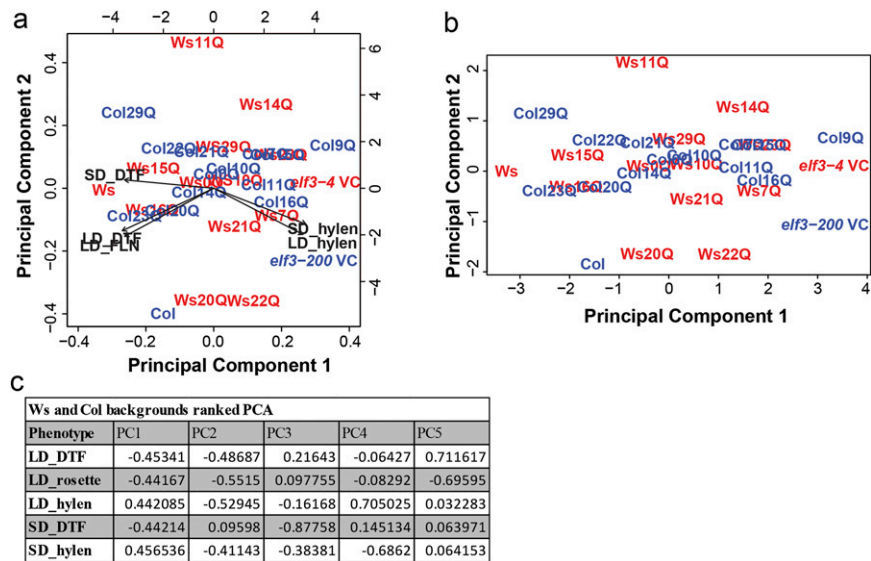


Fig. S5. The phenotypic effects of *ELF3-TR* copy number variation are strongly background-dependent. PCA of phenotypic data from all *ELF3-TR* alleles in both *elf3-4* (Ws accession) and *elf3-200* (Col accession) backgrounds. (A) Biplot of PC1 and PC2, graphically showing the contribution of phenotypes to PCs as black arrows. Note that for the biplot representation, PC1 and PC2 are transformed to the same scale (bottom and left axes), whereas phenotype contributions (in red) are allowed to differ in scale (top and right axes). Phenotypes are hypocotyl length in short and long days (SD_hylen and LD_hylen), DTF in short and long days (SD_DTF and LD_DTF), and FLN in long days (LD_FLN). Wild-type plants are characterized by late flowering (large SD and LD_DTF, many rosette leaves) and short hypocotyls (small SD and LD_hylen), relative to *elf3* loss-of-function mutants. Text in red represents a given allele in the Ws background (transgenics in *elf3-4*), and text in blue represents alleles in the Col background (transgenics in *elf3-200*). (B) PC1 and PC2. (C) PCA loadings for both backgrounds. hylen = hypocotyl length (mm). PCA loadings describe the composition of a principal component [i.e., the contribution of each phenotype in calculating the principal component, and the direction of a phenotype's contribution (the sign of the loading)]. For PC1, flowering-time phenotypes and circadian clock phenotypes have opposite loading signs, describing the tendency of late-flowering plants to have short hypocotyls (and short petioles; i.e., to be wild-type for all phenotypes).

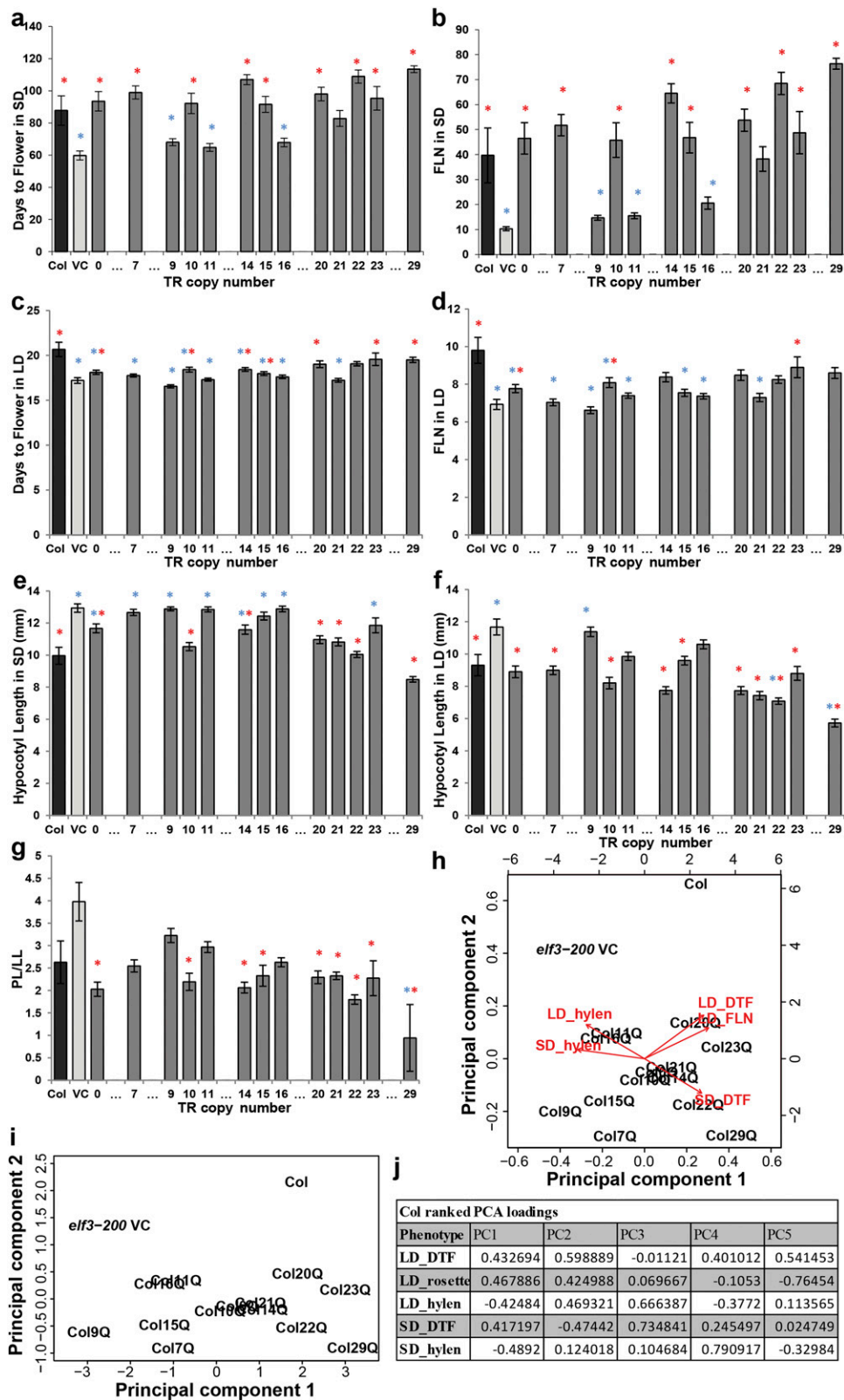


Fig. S6. *ELF3-TR* variation has nonlinear phenotypic effects in the *elf3-200* background (Col-0 accession). (A) DTF under SD ($n = 9$ plants/line). (B) FLN under SD ($n = 9$ plants per line). (C) DTF under LD ($n = 15$ plants per line). (D) FLN under LD ($n = 15$ plants per line). (E) Hypocotyl length under SD ($n = 20$ – 30 seedlings per line). (F) Hypocotyl length under LD ($n = 20$ – 30 seedlings per line). (G) PL/LL ratio under SD ($n = 9$ plants per line). Data are from the same plants as in B. *ELF3-TR* alleles are indicated with the number of Qs encoded, Col is wild-type, VC is the *elf3-200* vector control (VC). Blue and red asterisks indicate alleles that are significantly different from the wild-type and from the vector control, respectively, by Tukey-HSD test ($\alpha = 0.05$). Bars indicate \pm SEM. These experiments were repeated at least once with similar results. (H and I) PCA of phenotypic data for all *ELF3-TR* alleles in the *elf3-200* (Col accession) background. (H) Biplot of PC1

Legend continued on following page

Table S1. Cont.

Accession	<i>ELF3</i> TR copy number
GOT-7	16
Gr-1	21
Gu-0 (=Gue-0)	19
Gul-1-2	11
Gy-0	19
H55	7
Hi-0	16
Hod	12
Hov-4-1	16
Hovdala-2	16
HR-10	14
HR-5	19
Hs-0	16
Hsm	11
In-0	16
Is-0	17
Jm-0	11
K _a -0	19
Kas-1	16
Kas-2	29
Kavlinge-1	9
Kent	11
Kin-0	19
Kni-1	19
Knox-10	16
Knox-18	14
Koln	12
Konchezero (N13)	16
Kondara	14
KZ-1	21
Kz-13	14
Kz-9	14
Lc-0	19
Ler-1	17
Liarum	16
Lillo-1	21
Lip-0	15
Lis-1	15
Lis-2	13
LL-0	13
Lm-2	19
Lom-1-1	11
Lov-1	16
Lov-5	16
LP2-2	26
LP2-6	21
Lu-1	13
Lz-0	9
Mr-0	24
Mrk-0	13
MS-0	15
Mt-0	21
Mz-0	14
N6034	14
N6187	19
Na-1	22
NC-6	14
Nd-1	16
NFA-10	18
NFA-8	14
Nok-3	16
Nw-0	14

Table S1. Cont.

Accession	<i>ELF3</i> TR copy number
Ws	16
Ws-0	21
Ws-2	16
Wt-5	14
Yo-0	16
Zdr-1	13
Zdr-6	17

Table S2. Independent *A. thaliana* T₃ and T₄ homozygous lines: Transgenic plants in the *elf3-4* background

TR copy number	Line	Expression relative to Ws wild-type	CV of expression
Vector only	V1-1	0.45	0.04
0	0R1-3	4.18	0.01
0	0R4-3	3.08	0.02
0	0R5-3	1.58	0.01
7	7R3-1	2.38	0.02
7	7R5-2	0.86	0.01
10	10R1-1	2.41	0.01
10	10R2-2	1.49	0.01
10	10R4-2	2.13	0.01
11	11R1-3	2.17	0.03
11	11R2-3	1.65	0.01
11	11R8-1	0.81	0.02
11	11R9-1	2.35	0.03
14	14R1-1	0.99	0.01
14	14R4-2	1.81	0.01
15	15R1-2	2.68	0.01
15	15R2-1	2.31	0.02
15	15R3-1	3.40	0.01
16	16R1-2	1.86	0.01
16	16R4-2	2.14	0.01
16	16R6-2	3.82	0.02
16	16R7-2	2.35	0.02
16	16R8-1	0.97	0.02
16	16R10-3	0.89	0.01
20	20R1-2	1.20	0.02
20	20R2-1	0.95	0.02
20	20R3-2	1.28	0.02
21	21R2-2	0.97	0.01
21	21R3-2	3.81	0.01
21	21R5-3	3.69	0.01
22	22R3-3	4.53	0.01
22	22R6-1	1.35	0.01
22	22R8-1	3.29	0.01
23	23R2-1	3.30	0.02
23	23R5-1	0.98	0.00
29	29R3-2	1.29	0.00
29	29R4-1	2.01	0.02
29	29R5-2	1.21	0.02

Three technical replicates were used to obtain expression values. The CV of expression was calculated as:

$$CV = \sqrt{cv_{ELF3}^2 + cv_{UBC}^2}$$

Table S4. Independent *A. thaliana* T₃ and T₄ homozygous lines: Transgenic plants in the *elf3-200* background

TR copy number	Line	Expression relative to Col-0 wild-type	SE of expression
Vector only	V1-1	0.05	0.00
0	0R1-1	3.48	0.12
0	0R3-1	2.54	0.32
0	0R5-1	3.42	0.42
7	7R3-1	2.33	0.20
7	7R4-3	2.21	0.33
7	7R5-1	1.44	0.03
9	9R2-1	0.27	0.02
9	9R4-1	0.73	0.10
9	9R5-1	1.63	0.21
10	10R1-2	1.74	0.01
10	10R3-3	2.74	0.09
10	10R7-3	2.04	0.25
11	11R3-1	1.38	0.09
11	11R5-4	1.52	0.16
11	11R6-1	1.63	0.21
11	11R7-1	0.61	0.03
14	14R3-4	2.10	0.13
14	14R5-4	2.24	0.00
14	14R10-3	1.59	0.49
15	15R2-2	1.59	0.27
15	15R4-2	1.81	0.08
15	15R8-1	0.53	0.34
16	16R1-1	0.49	0.00
16	16R2-4	2.01	0.12
16	16R3-2	1.37	0.36
16	16R4-2	1.97	0.17
20	20R1-2	4.27	0.39
20	20R2-3	0.81	0.02
20	20R3-3	3.07	0.17
20	20R5-3	3.49	0.57
21	21R1-2	3.05	0.13
21	21R3-2	1.25	0.04
22	22R3-3	3.34	0.26
22	22R4-2	1.37	0.35
22	22R6-1	2.69	0.10
22	22R7-2	2.59	0.54
23	23R2-4	0.39	0.12
23	23R4-3	1.79	0.03
29	29R4-2	0.81	0.21
29	29R11-1	3.75	0.60

At least two biological replicates with three technical replicates each were used to obtain expression values. The SE of expression was calculated as:

$$SE = \frac{Std.Dev.}{\sqrt{n}}$$

Table S5. Primer sequences: Cloning and mutagenesis primers

Primer name	Sequence
Nar1 Sense	GAGATCTGATAATGAACCGGCCACAGCAACAGCAACAG
Nar1 Antisense	TGTTGCTGTTGCTGTGGCGCCGTTTCATTATCAGATCTC
Nco1 Sense	CTCAATATCACCCCGCCATGGGATCCACC
Nco1 Antisense	GGTGGGAATCCCATGGCGGGTGATATTGAG
PolyQ Sense	CCCTTCCCATGGGATCCACCTCTGTGAAT
PolyQ Antisense	TTTTGGGGCGCCGGTTCATTATCAGATCTCTG
OQ Sense	ACCATAATGAACCCATATTGTTCAAGCCCCAATGAGCAAATGAACCAAGTTTGGGA
OQ Antisense	TCCAAACTGGTTCATTGCTCATTGGGGCTTGAACAATATGGGTTTCATTATGGT
ELF3 Construct S	CAATAATGGTTTCTGACGTA
ELF3 Construct A	ACCAATGGTACTCAAATAGTTTGGTCATACGG

